

# Evaluation of carbonation service life of slag blended concrete considering climate changes

Xiao-Yong Wang\*<sup>1</sup> and Yao Luan<sup>2a</sup>

<sup>1</sup>Department of Architectural Engineering, Kangwon National University, Chuncheon-si, Korea

<sup>2</sup>Department of Civil and Environmental Engineering, Saitama University, Saitama, Japan

(Received July 3, 2017, Revised November 21, 2017, Accepted December 13, 2017)

**Abstract.** Climate changes, such as increasing of CO<sub>2</sub> concentration and global warming, will impact on the carbonation service life of concrete structures. Moreover, slag blended concrete has a lower carbonation resistance than control concrete. This study presents a probabilistic numerical procedure for evaluating the impact of climate change on carbonation service life of slag blended concrete. This numerical procedure considers both corrosion initiation period and corrosion propagation period. First, in corrosion initiation period, by using an integrated hydration-carbonation model, the amount of carbonatable substances, porosity, and carbonation depth are calculated. The probability of corrosion initiation is determined through Monte Carlo method. Second, in corrosion propagation period, a probabilistic model is proposed to calculate the critical corrosion degree at surface cracking, the probability of surface cracking, and service life. Third, based on the service life in corrosion initiation period and corrosion propagation period, the whole service life is calculated. The analysis shows that for concrete structures with 50 years service life, after considering climate changes, the service life reduces about 7%.

**Keywords:** slag blended concrete; climate change; service life; carbonation; probabilistic model

## 1. Introduction

Carbonation is a key factor of the deterioration of reinforced concrete in atmospheric environments. Carbonation makes pH of capillary pore solution to decrease, destroys the passive layer of steel rebar surface, and reduces the service life of concrete structures. Moreover, slag is increasingly used in concrete industry for producing high-performance concrete. Slag blended concrete has a higher carbonation depth than control concrete (Gruyaert *et al.* 2013). Furthermore, climate changes, such as increase of CO<sub>2</sub> concentration and environmental temperature, will accelerate the rate of CO<sub>2</sub> penetration and steel corrosion (Damtoft *et al.* 2008). Consequently, the service life of concrete will be reduced. Hence the evaluation of service life considering the effect of climate change is crucial for carbonation durability design of slag blended concrete.

Numerous experimental and theoretical studies have been done about carbonation and service life of concrete structures. Sulapha *et al.* (2003) experimentally found that the concrete containing mineral admixtures generally had lower resistance to carbonation due to the reduction of calcium hydroxide. Sisomphon and Franke (2007) experimentally found that for concrete containing high volume mineral admixtures, the rate of carbonation declined

with curing age. Khunthongkeaw *et al.* (2006) experimentally found that high calcium fly ash blended concrete had better carbonation resistance than low calcium fly ash blended concrete. Except for aforementioned experimental studies, some theoretical studies have been done about concrete carbonation. Papadakis (2000, 2007) proposed a computer-aided approach evaluating the carbonation depth and service life of concrete structures. Papadakis' carbonation model was valid for both Portland cement concrete and supplementary cementitious materials (SCMs) blended concrete. Isgor and Razaqpur (2004) made a finite element model considering the interactions among heat transfer, moisture transport, and carbonation. Kwon and Na (2011) used a probabilistic approach for evaluating service life of concrete columns with cracks and joint. However, the aforementioned theoretical studies mainly focused on the corrosion initiation process. The corrosion propagation period after carbonation was not considered. Garcia-Segura *et al.* (2014) analyzed the service life of concrete structures considering both initiation of corrosion and propagation of corrosion. Marques *et al.* (2012, 2013) proposed probabilistic methods for modeling the initiation period and propagation period due to carbonation and chloride ingress. But both studies did not consider the effects of climate changes on CO<sub>2</sub> ingress and service life of concrete structures.

Regarding the effects of climate change on carbonation, some numerical models are proposed. Yoon *et al.* (2007) analyzed the increase of CO<sub>2</sub> concentration on carbonation of concrete. Climate scenario IS92a was used for describing time-dependent CO<sub>2</sub> concentration. Talukdar *et al.* (2012, 2014) evaluated the service life of concrete structures considering different climate change scenarios. However,

\*Corresponding author, Professor  
E-mail: wxbrave@kangwon.ac.kr

<sup>a</sup>Professor  
E-mail: luanyao@mail.saitama-u.ac.jp

Yoon *et al.* (2007), Talukdar *et al.* (2012, 2014)'s methods do not consider the probabilistic distribution of material properties and environmental conditions. Bastidas-Arteaga (2013), Larrarda (2014), Kolio (2014) proposed probabilistic approaches to estimate the service life of concrete structures considering the influence of global warming. Peng and Stewart (2014, 2016) made spatial time-dependent reliability analysis of climate changes and corrosion damage risks for concrete structures in different countries, such as China and Australia. But former studies mainly focused on the service life of Portland cement concrete. The effect of supplementary cementitious materials, such as slag, on service life, is not considered. In addition, although former studies calculate the service life taking into account the climate change, former studies do not give a clear answer about the extent of service life reduction for various concrete mixing proportions and cover depths. To obtain the clear answer of the extent of service life reduction, a quantitative regression analysis about relative service life is carried out in this study. Based on this quantitative regression analysis, we provide a clear answer about the extent of service life reduction for various concrete mixing proportions and cover depths.

To overcome the weak points of former studies, this study presents a probabilistic numerical procedure for evaluating the impact of climate change on the service life of concrete subjected to carbonation. The proposed numerical procedure is valid for both Portland cement concrete and slag blended concrete. The whole service life is determined as the sum of corrosion initiation period and corrosion propagation period. The ratio of service life with climate change to that without climate change is quantitatively analyzed.

## 2. Carbonation service life model of slag blended concrete

### 2.1 Corrosion initiation period due to carbonation

Carbonation of concrete is a complicated physicochemical process which relates to both concrete materials properties and environmental conditions. In our former study, Wang and Lee (2010) proposed a hydration-carbonation integrated model for slag blended concrete. The amounts of carbonatable substances and porosity of concrete are calculated from the kinetic hydration model, and the calculated results from the hydration model are used as input parameters for the carbonation model. Furthermore, the carbonation depth is calculated considering concrete constitutes and exposure conditions. The hydration-carbonation integrated model considered the influences of water to binder ratio, supplementary cementitious materials (SCMs) replacement ratio, and curing period on concrete carbonation.

Compared with carbonation models in literature, the hydration-carbonation integrated model proposed in this study shows some advantages: First, this study considers the effects of water-to-binder ratio and slag additions on reaction degree of binders. Carbonation models shown in

references (Papadakis 2000 and 2007, Isgor and Razaqpur 2004) assume that binders completely hydrates (reaction degree of binders is 100%) regardless of the water to binder ratios. While Bentz (1997, 2005) found that when water-to-cement ratio decreases, the rate of hydration and final degree of hydration decreases. Second, this study takes into account the influences of slag additions on carbonatable substances contents, concrete porosity, and corrosion current. Carbonation models in references (Yoon *et al.* 2007, Kwon and Na 2011, Talukdar *et al.* 2012, 2014, Bastidas-Arteaga *et al.* 2013, Larrarda *et al.* 2014, Kolio *et al.* 2014, Peng and Stewart 2014, 2016) do not consider the effect of SCMs on carbonation and steel corrosion. Third, this study considers the effect of time-varying boundary condition on concrete carbonation. Carbonation models in references (Garcia-Segura *et al.* 2014, Marques *et al.* 2012, 2013) do not consider time-varying boundary conditions, such as time-dependent  $\text{CO}_2$  concentration and environmental temperature.

The carbonatable substances in concrete are calcium hydroxide (CH) and calcium silicate hydrate (CSH). For slag blended concrete, the amount of CH is dependent on both hydration of cement and reaction of slag. The amount of CH can be determined as follows

$$CH(t) = CH_{CE} * C_0 * \alpha - v_{SG} * P * \alpha_{SG} \quad (1)$$

where  $CH_{CE}$  is the mass of CH produced from unit mass of cement,  $C_0$  ( $\text{kg}/\text{m}^3$ ) is mass of cement in the mixing proportions,  $\alpha$  is degree of cement hydration,  $P$  ( $\text{kg}/\text{m}^3$ ) is mass of slag in the mixing proportions,  $v_{SG}$  is the stoichiometric ratio of slag to CH ( $v_{SG} = 0.25 - 0.1 * \frac{P}{P + C_0}$ ), this

equation is obtained based on the analysis of calcium hydroxide content and adiabatic temperature rise of concrete containing different slag contents (Wang and Lee 2010)), and  $\alpha_{SG}$  is reaction degree of slag. Hydration degree of cement  $\alpha$  can be determined as  $\alpha = \int_0^t \frac{d\alpha}{dt} dt$  where  $\frac{d\alpha}{dt}$  is the rate of cement hydration. Similarly, reaction degree of slag  $\alpha_{SG}$  can be determined as  $\alpha_{SG} = \int_0^t \frac{d\alpha_{SG}}{dt} dt$  where  $\frac{d\alpha_{SG}}{dt}$  is the rate of slag reaction. The detailed equations about calculating the rate of cement hydration and slag reaction are available in our former studies (Wang and Lee 2010).

Both Portland cement hydration and slag reaction produce CSH. The CSH produced from slag reaction has a lower Ca/Si ratio than that produced from cement hydration. Bentz (1997, 2005) proposed that compound formula of CSH produced from hydration of cement is  $\text{C}_{1.7}\text{SH}_4$ , and that of CSH produced from slag reaction is  $\text{C}_{1.35}\text{SH}_{5.53}$ . The S in cement and slag forms CSH (Papadakis 2000 and 2007). The CSH content in slag blended concrete can be determined as follows (Wang and Lee 2010)

$$CSH(t) = CSH_c(t) + CSH_{SG}(t) \quad (2)$$

$$CSH_c(t) = 3.79 * f_{s,c} * C_0 * \alpha \quad (3)$$

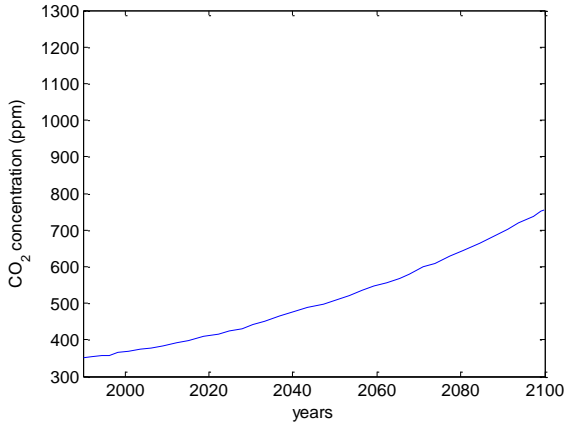
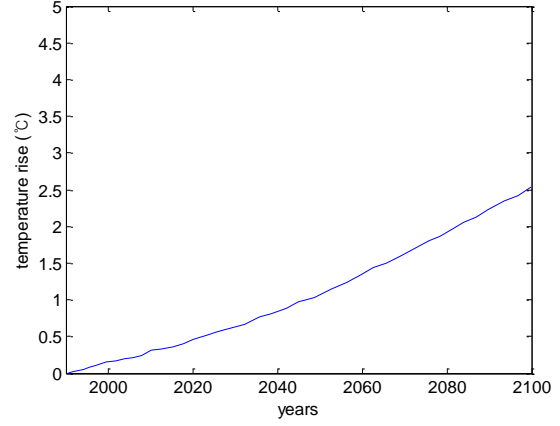

 Fig. 1 CO<sub>2</sub> concentration rise


Fig. 2 Temperature rise

$$CSH_{SG}(t) = 3.91 * f_{S,P} * P * \alpha_{SG} \quad (4)$$

where  $CSH_C$  ( $\text{kg/m}^3$ ) is the content of CSH produced from cement hydration,  $CSH_{SG}$  ( $\text{kg/m}^3$ ) is the content of CSH produced from slag reaction,  $f_{S,C}$  is S content in cement, and  $f_{S,P}$  is S content in slag. The coefficient 3.79 in Eq. (3) is the mass ratio of  $C_{1.7}SH_4$  to S in  $C_{1.7}SH_4$ . The coefficient 3.91 in Eq. (4) is the mass ratio of  $C_{1.35}SH_{5.53}$  to S in  $C_{1.35}SH_{5.53}$ .

Concrete porosity decreases due to the filling the pore space from reaction products of cement hydration, slag reaction, and carbonation. The concrete porosity can be calculated as follows

$$\varepsilon = \frac{W_0 - 0.25 * C_0 * \alpha - 0.3 * P * \alpha_{SG} - \Delta \varepsilon_C}{\rho_w} \quad (5)$$

where  $\varepsilon$  is porosity,  $W_0$  ( $\text{kg/m}^3$ ) is the mass of water in mixing proportions,  $\rho_w$  ( $\text{kg/m}^3$ ) is the density of water,  $0.25 * C_0 * \alpha$  ( $\text{kg/m}^3$ ) means the porosity reduction due to cement hydration,  $0.3 * P * \alpha_{SG}$  ( $\text{kg/m}^3$ ) means the porosity reduction due to slag reaction, and  $\Delta \varepsilon_C$  means the porosity reduction due to carbonation (Papadakis 2000 and 2007). Papadakis (2000 and 2007) proposed the changing of molar volume of carbonatable substances due to carbonation. Based on the contents of carbonatable substances and the changing of molar volume, the reduction of porosity of concrete due to carbonation can be calculated. In addition, carbonation in concrete containing SCMs can reduce pore connectivity and change in the pore structure. The current study only considers the reduction of porosity, and the changing of distribution of pore structure remains a matter of future study for more precise prediction.

Carbonation is significantly influenced by concrete relative humidity (RH). Carbonation of concrete tends to be highest for the environmental relative humidity of 50%-70%. When the relative humidity is less than 50%, there is no sufficient moisture for the progress of carbonation reaction. For a relative humidity higher than 70%, the diffusion of  $CO_2$  is hindered due to the increase of saturation degree of concrete pores. Papadakis *et al.* (2000 and 2007) proposed that for usual range of environmental condition ( $RH > 0.55$ ), carbonation is controlled by diffusion of  $CO_2$  in concrete. The concrete carbonation depth can be calculated as follows (Papadakis *et al.* 2000, 2007)

$$x_c = \sqrt{\frac{2D_C[CO_2]_0 t}{[CH] + 1.7[CSH]_C + 1.35[CSH]_{SG}}} \quad (6)$$

$$D_C = A \left( \frac{\varepsilon}{\frac{C_0}{\rho_c} + \frac{P}{\rho_{SG}} + \frac{W_0}{\rho_w}} \right)^a \left( 1 - \frac{RH}{100} \right)^{2.2} \quad (7)$$

where  $x_c$  (m) is concrete carbonation depth,  $D_C$  ( $\text{m}^2/\text{s}$ ) is the diffusivity of  $CO_2$  in carbonated concrete,  $[CO_2]_0$  ( $\text{mol/m}^3$ ) is the  $CO_2$  concentration in exposure environment,  $\rho_c$  ( $\text{kg/m}^3$ ) is the density of cement,  $\rho_{SG}$  ( $\text{kg/m}^3$ ) is the density of slag,  $A$  ( $\text{m}^2/\text{s}$ ) and  $a$  are parameters of  $CO_2$  diffusivity, and  $RH$  is relative humidity of exposure environment. The denominator of Eq. (6)  $[CH] + 1.7[CSH]_C + 1.35[CSH]_{SG}$  denotes the contents of carbonatable substances in concrete. In Eq. (7), the values of parameters  $A$  and  $a$  are intrinsic constants of concrete and their values do not change when concrete mixing proportions or environmental conditions change. Because Eq. (6) is not in difference scheme, Eq. (6) is only valid for concrete with constant exposure conditions and materials properties. However, if Eq. (6) is transformed into difference scheme, it can be used to calculate carbonation depth of concrete with time-dependent exposure conditions and materials properties.

Climate models project the response of numerous climate variables, such as global environmental temperature and sea level, to different scenarios of greenhouse gas emission and other human-related emissions. Among these different scenarios, IS92a scenario, which is put forward by the Intergovernmental Panel on Climate Change (IPCC) (Houghton *et al.* 2001), is considered as one of the best models for climate change. IS92a global climate change scenario proposes that in the 21st century,  $CO_2$  concentration will increase from 350 ppm to 750 ppm (shown in Fig. 1), and the average temperature increases about  $2.5^\circ\text{C}$  (shown in Fig. 2).

Climate changes, such as the  $CO_2$  concentration increase and environmental temperature increase, will accelerate carbonation of concrete. Eq. (6) does not consider the time-dependent  $CO_2$  concentration and environmental temperature. To considering the time-dependent  $CO_2$  concentration and environmental temperature, Eq. (6) can be transformed

using the difference scheme (similar to taking the derivative) as follows

$$dx_c = CR \frac{1}{2\sqrt{t}} dt \quad (8)$$

$$CR = \sqrt{\frac{2[CO_2(t)]D_C(t)}{[CH] + 1.7[CSH]_C + 1.35[CSH]_{SG}}} \quad (9)$$

where  $dx_c$  is the increase of carbonation depth in time increment  $dt$  and  $CR$  is carbonation rate parameter. In Eq. (9),  $D_C$  and  $[CO_2]_0$  are functions of time. We approximately assumed that in each time step, the values of  $D_C$  and  $[CO_2]_0$  can be regarded as constants.

With the increase of environmental temperature,  $CO_2$  diffusivity increases. Kwon and Na (2011) proposed the dependence of  $CO_2$  diffusivity on temperature can be described using Arrhenius's Law as follows

$$D(T) = D_{ref} \exp \left[ \beta \left( \frac{1}{T_{ref}} - \frac{1}{T} \right) \right] \quad (10)$$

where  $D_{ref}$  ( $m^2/s$ ) is  $CO_2$  diffusivity at a reference temperature, and  $\beta$  is activity energy of  $CO_2$  ( $\beta=4300$ ),  $T_{ref}$  ( $20^\circ C$ ) is reference temperature.

In the stage of corrosion initiation, the durability failure criterion is that carbonation depth exceeds the cover depth. The evaluations of carbonation depth involve various uncertainties which consist of physical uncertainties, statistical uncertainties, model uncertainties, and decision uncertainties (Kwon and Na 2011). Considering the various uncertainties of carbonation depth prediction, the durability failure probability can be calculated by using Monte Carlo method as follows (Kwon and Na 2011)

$$g(t) = CV - x_c \quad (11)$$

$$p_{f1} = \frac{n(g(t) < 0)}{N} \quad (12)$$

where  $CV$  is the cover depth of concrete,  $g(t)$  is durability failure criterion,  $p_{f1}$  is the probability of carbonation durability failure.  $n(g(t) < 0)$  denotes the number of carbonation durability failure out of total  $N$  trials.

## 2.2 Corrosion propagation period after carbonation

After carbonation depth exceeds concrete cover depth, corrosion of steel rebar initiates. The rate of rebar corrosion is dependent on both concrete materials properties and exposure environments. Geng (2010) made experimental studies about the effects of environmental temperature, environmental relative humidity, water-to-cement ratio, and cover depth on corrosion current density. Stewart *et al.* (2011) estimated corrosion current density of concrete structures exposed to different carbonation environments. Based the experimental results from Geng (2010) and Stewart *et al.* (2011), an empirical equation for corrosion current density is written as follows (Geng 2010, Stewart *et al.* 2011)

$$i_s = 0.062 \left( \frac{RH}{0.45} \right)^{2.814} \left( \frac{T}{10} \right)^{0.466} \left( \frac{w/c}{0.35} \right)^{0.837} \left( \frac{CV}{10} \right)^{-0.436} \quad (13)$$

where  $i_s$  ( $\mu A/cm^2$ ) is corrosion current density, and  $w/c$  is the water-to-cement ratio. Eq. (13) shows that when relative humidity, temperature ( $^\circ C$ ) or water-to-cement ratio increase, corrosion current density increases. And when the cover depth increases, corrosion current density decreases. In Geng (2010)'s experimental study, the used cement was Portland cement. After 28 days standard curing, the experiments about measuring corrosion current density started. Eq. (13) does not consider the effect of slag on corrosion current. Parrott (1994) made an experimental study on carbonation-induced corrosion of slag blended concrete and Portland cement concrete. Parrott (1994) found that for carbonation-induced corrosion, slag blended concrete has a higher corrosion current than control Portland cement concrete. When slag is used to replace partially cement, because the rate of hydration of slag is much slower than that of cement, slag blended concrete has a higher porosity than plain concrete. The increase in concrete porosity and oxygen diffusivity will increase corrosion current density (Parrott 1994). Based on Parrott's experimental results about corrosion, an efficiency factor of slag for corrosion current density is proposed as 0.5 ( $w/c$  in Eq. (13) is written as  $w/(c+0.5slag)$ ). Corrosion propagation relates to both corrosion current density and other factors, such as concrete strength, cover depth, and steel diameter. Although slag blended concrete has a higher corrosion current density, it does not mean corrosion propagation in slag blended concrete is faster than OPC concrete because other factors also affect corrosion propagation.

By using corrosion current density and Faraday's law, the corroded depth of reinforced steel rebar can be determined as follows

$$\chi = \frac{i_s t M_F}{2.5 F \rho_F} \quad (14)$$

where  $\chi$  (m) is corroded depth,  $M_F$  (g/mol) is the atomic weight of corroded steel,  $F$  (C/mol) is Faraday constant, and  $\rho_F$  ( $kg/m^3$ ) is the density of corroded steel.

For carbonation-induced corrosion, corrosion of the steel rebar is not uniform. Generally, before surface cracking of concrete, corrosion occurs on the side of  $CO_2$  ingress. For the opposite side of  $CO_2$  ingress, corrosion of steel rebar is marginal. By using the corroded depth of steel rebar and considering non-uniform corrosion, the degree of corrosion can be calculated as follows

$$\eta = \frac{\chi}{R_0} \quad (15)$$

where  $\eta$  is the degree of corrosion of steel rebar, and  $R_0$  (m) is the radius of steel rebar. Eq. (15) is only valid before surface cracking of concrete occurs. Before surface cracking of concrete, corrosion occurs only on  $CO_2$  ingress side. After surface cracking of concrete, because the gas can ingress through the crack, corrosion will occur on both ingress side and the opposite side of  $CO_2$  ingress. When steel rebar has a very high degree of corrosion ( $\eta=1$ ), surface cracking of concrete occurs, and Eq. (15) is not valid for this condition.

After corrosion of steel rebar starts, corrosion products expand freely until the transition zone between steel rebar

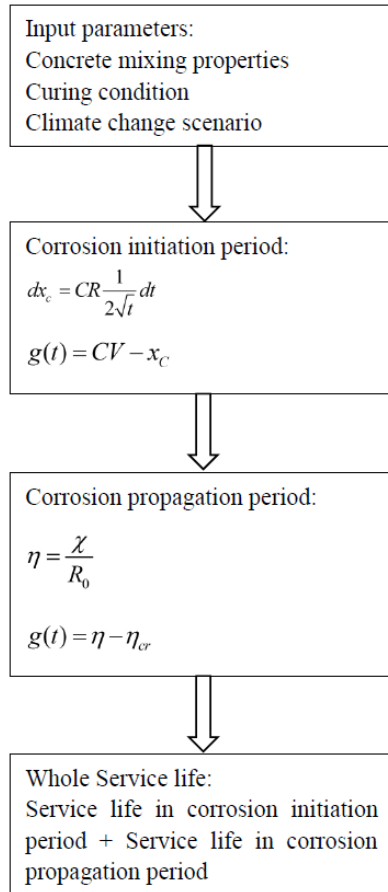


Fig. 3 Flow chart of service life prediction

and concrete is filled. Then the expansion pressure begins to develop in concrete around the steel rebar. Consequently tensile stress in surface concrete develops. Once the critical steel corrosion reached, cracking of surface concrete occurs. Wei *et al.* (2011) made finite element analysis about surface cracking of concrete induced from non-uniform corrosion. Based on analysis results from finite element analysis, Wei *et al.* (2011) proposed a regression equation for evaluating critical steel corrosion shown as follows

$$\eta_{cr} = \frac{4\delta_0 + 0.0624f_t^{0.91} \left(1 + \frac{CV}{2 * R_0}\right)^{1.98} (2R_0)^{0.96}}{(\rho - 1)(2R_0)} \quad (16)$$

where  $\eta_{cr}$  is critical steel corrosion,  $\delta_0$  ( $=12.5 \mu\text{m}$ ) is the depth of transition zone,  $f_t$  (MPa) is the tensile strength of concrete,  $\rho$  is the ratio of the volume of corrosion products to the volume of corroded steel.

In the corrosion propagation period, the durability failure criterion corresponds with the degree of corrosion exceeding the critical steel corrosion. The durability failure criterion in corrosion propagation period is shown as follows

$$g(t) = \eta - \eta_{cr} \quad (17)$$

Similarly, the probability of durability failure ( $g(t) > 0$ ) in corrosion propagation period  $p_{j2}$  also can be determined by using Monte-Carlo Method.

### 2.3 Summary of proposed model

Fig. 3 shows the flow chart of proposed model. The input parameters consist of concrete mixing proportions, curing conditions, and climate change scenario. In the corrosion initiation period, by using the hydration-carbonation integrated model, the carbonation depth is calculated considering time-dependent  $\text{CO}_2$  concentration and environmental temperature. Furthermore, the probability of corrosion initiation is determined using Monte-Carlo method. In the corrosion propagation period, based on critical steel corrosion and the progress of degree of corrosion, the probability of surface concrete cracking is determined.

In corrosion initiation period and corrosion propagation period, service life can be calculated based on the linear interpolation between time and durability failure probability. From corrosion initiation period to corrosion propagation period, a failure of the system may cause more severe consequences, the reliability index should increase, and the failure probability corresponding to service life should decrease (Kwon and Na 2011). As proposed by FIB (2006), for residential and office buildings with a consequences class CC2, the reliability index in initiation period and corrosion propagation period are 1.3 and 1.5 respectively. The failure probability corresponding to service life in initiation period is 10%, and the failure probability corresponding to service life in corrosion propagation period is 7% (FIB 2006). The whole service life is the sum of service life in corrosion initiation period and corrosion propagation period.

## 3. Analysis of carbonation service life of slag blended concrete

### 3.1 Verification of carbonation model

Experimental results from Parrott (1996) are adopted to verify the proposed carbonation model for slag blended concrete. Parrott (1996) measured natural carbonation depth of slag blended concrete with different slag contents 25%, 50%, and 75%. The water to binder ratio was 0.59, and the binder content was  $320 \text{ kg/m}^3$ . After three days or 28 days sealed curing, the cubic concrete specimens were put in natural carbonation environment with 60% relative humidity and  $20^\circ\text{C}$ .  $\text{CO}_2$  concentration in lab air was 0.039%. After 6 and 18 months exposure, the natural carbonation depth was measured.

By using the hydration model, CH content, CSH content, and concrete porosity are calculated and shown in Fig. 4. As shown in Fig. 4(a), for Portland cement concrete, CH content increases continuously since early ages. For 50% slag blended concrete, CH contents initially increase, because the production of CH from cement hydration is dominant. After reaching a peak value, CH content begins to decrease, because the consumption of CH from slag reaction is dominant. As shown in Fig. 4(b), for 50% slag blended concrete, the total CSH content is the sum of CSH produced from cement hydration and CSH produced from slag reaction. In the early-age, the total CSH content of

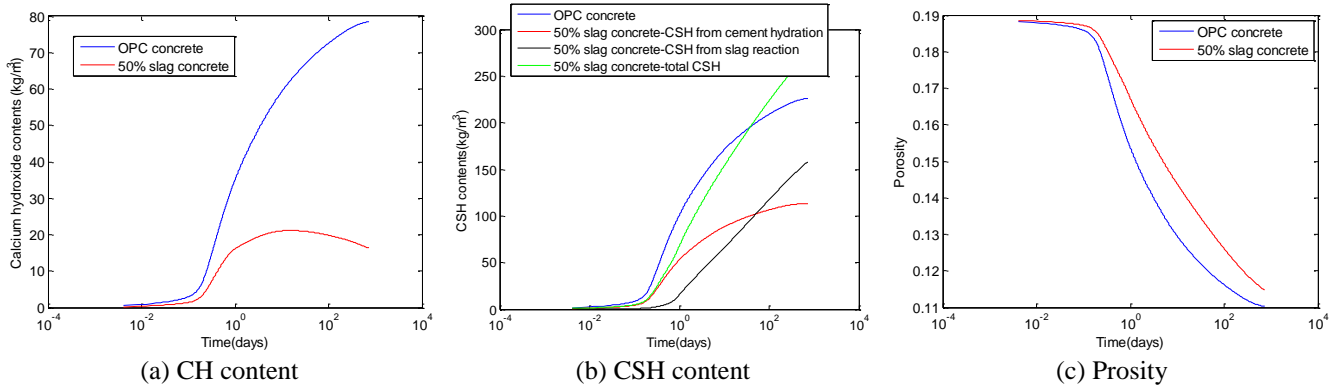


Fig. 4 properties evaluation of slag blended concrete

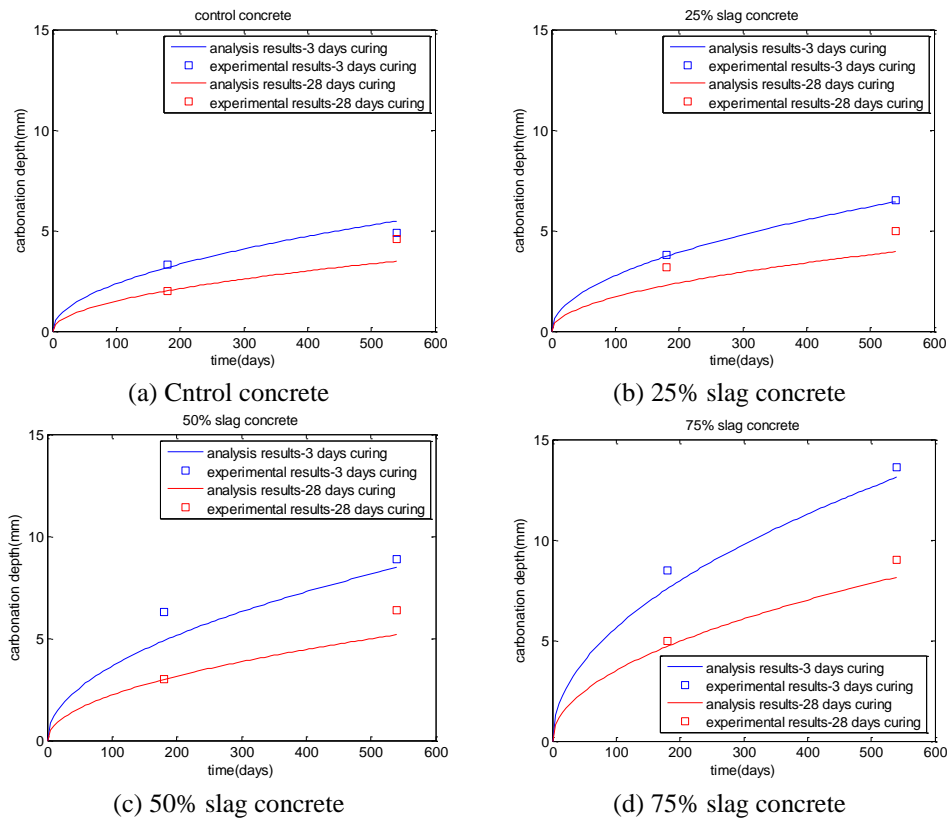


Fig. 5 Carbonation depth of slag blended concrete

blended concrete is lower than that of control concrete. And in the late-age, due to the propagation of slag reaction, CSH content of slag blended concrete exceeds that of control concrete. As shown in Fig. 4(c), slag blended concrete has a higher porosity than that of control concrete. This is because the rate of hydration of slag is much slower than that of cement.

The calculation results from cement hydration model, such as CH content, CSH content, and porosity are used as input parameters for carbonation model. Carbonation occurs at the surface zone of concrete, and the relative humidity in the carbonated zone approximately equals to that in exposure environment. When the environmental relative humidity is less than 80%, the hydration of concrete stops. Hence further hydration of concrete during carbonation tests is ignored in this study (this assumption is also used in

section 3.2). Based on the experimental results of carbonation depths of concrete with different slag replacement levels and pre-curing periods before carbonation tests, the intrinsic parameters of  $\text{CO}_2$  diffusivity are calibrated as  $A=8.44e-6$ ,  $a=4.4$ . The values of intrinsic parameters  $A$  and  $a$  do not change when concrete mixing proportions or curing periods change. In Papadakis' study (2000), based on the carbonation depths of concrete containing different SCMs, Papadakis calibrated the values of  $A$  and  $a$  as  $6.1e-6$  and 3 respectively. The values of  $A$  and  $a$  in our study general agree with those in Papadakis' study. The carbonation depth of slag blended concrete is calculated and shown in Fig. 5. When the slag contents decrease or curing periods before carbonation tests increase, carbonation depths of concrete decrease. Gruyaert *et al.* (2013) also found similar experimental results for concrete

Table 1 listing of parameters for service life evaluation

Concrete Materials properties					Environmental conditions			
Water to binder ratios	concrete Cover depth	Moist curing periods	Binder contents (kg/m <sup>3</sup> )	slag replacement ratio	Diameter Of steel rebar(mm)	Relative humidity	Initial Temperature (°C)	Initial time
0.5, 0.6	30 mm, 40 mm	28 days	320	0.25,0.50,0.75	16	0.6	20	2000 year

Table 2 statistical parameters

Parameter	Mean	Coefficient of variance	Distribution
concrete cover depth (CV)	30 mm 40 mm	0.2 (Kwon and Na 2011)	Normal
carbonation rate parameter (CR)	$CR = \sqrt{\frac{2[CO_2(t)]_0 D_{CO_2}(t)}{[CH] + 1.7[CSH]_c + 1.35[CSH]_{SG}}}$	0.15 (Kwon and Na 2011)	Normal
28 days Compressive strength (MPa) $f_{c28}$	$f_c(t) = 53.16 * \frac{CSH_c(t)}{W_0} + 47.03 * \frac{CSH_{SG}(t)}{W_0} - 11.63$	0.15 (Geng 2010)	normal
28 days tensile strength (MPa)	$0.69 \sqrt{f_{c28}}$	0.15 (Geng 2010)	normal
Rate of corrosion ( $\mu A/cm^2$ )	$i_s = 0.062 \left(\frac{RH}{0.45}\right)^{2.814} \left(\frac{T}{10}\right)^{0.466} \left(\frac{w/c}{0.35}\right)^{0.837} \left(\frac{CV}{10}\right)^{-0.436}$	0.5 (Stewart <i>et al.</i> 2011)	lognormal
CO <sub>2</sub> concentration	[CO <sub>2</sub> (t)]	COV <sub>max</sub> (t)=0.06 (Stewart <i>et al.</i> 2011)	normal
temperature	$\Delta T + 20$	COV <sub>max</sub> (t)=0.06 (Stewart <i>et al.</i> 2011)	normal

with different slag additions and curing periods. Slag additions and reduction of curing periods will increase the carbonation depth of concrete (Gruyaert *et al.* 2013).

### 3.2 Service life in corrosion initiation period

Carbonation service life of concrete is dependent on various parameters, such as materials properties and environmental conditions. In this study, parameter studies are performed for analyzing the influences of climate change on carbonation service life of concrete. Listing of parameters is shown in Table 1. Two levels of water-to-binder ratios (W/B: 0.5 and 0.6), two levels of concrete cover depths (CV: 30 mm and 40 mm), and three levels of slag replacement ratios ( $P/(C_0+P)$ : 0.25,0.5, and 0.75) are adopted in the parameter analysis. The relative humidity of exposure environment is assumed as 60% (this is constant over all the years), the initial temperature is 20°C, and the initial time of calculation is the year 2000. The time-dependent CO<sub>2</sub> concentration and temperature increase are presented in Fig. 1 and Fig. 2 respectively. The statistical parameters are shown in Table 2. The uncertainties of concrete cover depth, carbonation rate parameter, the strength of concrete, the rate of corrosion, CO<sub>2</sub> concentration, and temperature are considered. The compressive strength of slag blended concrete is evaluated using kinetic blended hydration model in our former study (Wang 2010). As time increases, the coefficients of variance of CO<sub>2</sub> concentration and temperature also increase (Stewart *et al.* 2014). At the initial time, the coefficients of variance are zero; and after 100 years exposure, the coefficients of variance are 0.06 (Stewart *et al.* 2014).

By using the integrated hydration-carbonation model,

the carbonation depth of concrete can be determined. Moreover, using Monte Carlo method, the probability of corrosion initiation of steel rebar can be calculated. Fig. 6 shows the probability of corrosion initiation considering the effect of climate change. Climate change makes the probability of corrosion initiation increase. Slag blended concrete has a higher probability of corrosion initiation than control concrete (from Fig. 6(a) to Fig. 6(b)). When concrete cover depth increases, the probability of corrosion initiation decreases (from Fig. 6(b) to Fig. 6(c)). When slag replacement ratio increases, the probability of corrosion initiation increases (from Fig. 6(c) to Fig. 6(e)). When water to binder ratio decreases, the probability of corrosion initiation decreases (From Fig. 6(b) to Fig. 6(f)).

In initiation period, the service life is the time required to achieve failure probability 10%. Based on the relation between time and probability of corrosion initiation, the service life of concrete can be calculated. In this study, former service life is defined as service life without climate change, revised service life is defined as service life with climate change, and relative service life means the ratio of revised service life to former service life. Table 3 shows the service life in corrosion initiation period. When former service life increases, relative service life decreases. This is because CO<sub>2</sub> concentration and temperature monotonically increase with time (shown in Fig. 1 and Fig. 2). Fig. 7 shows the relative service life as a function of former service life. Relative service life approximately linearly decreases with the increase of former service life. The slope of linear regression equation about relative service life is -0.0036 (relative service life=1-0.0036\*former service life).

### 3.3 Service life in corrosion propagation period

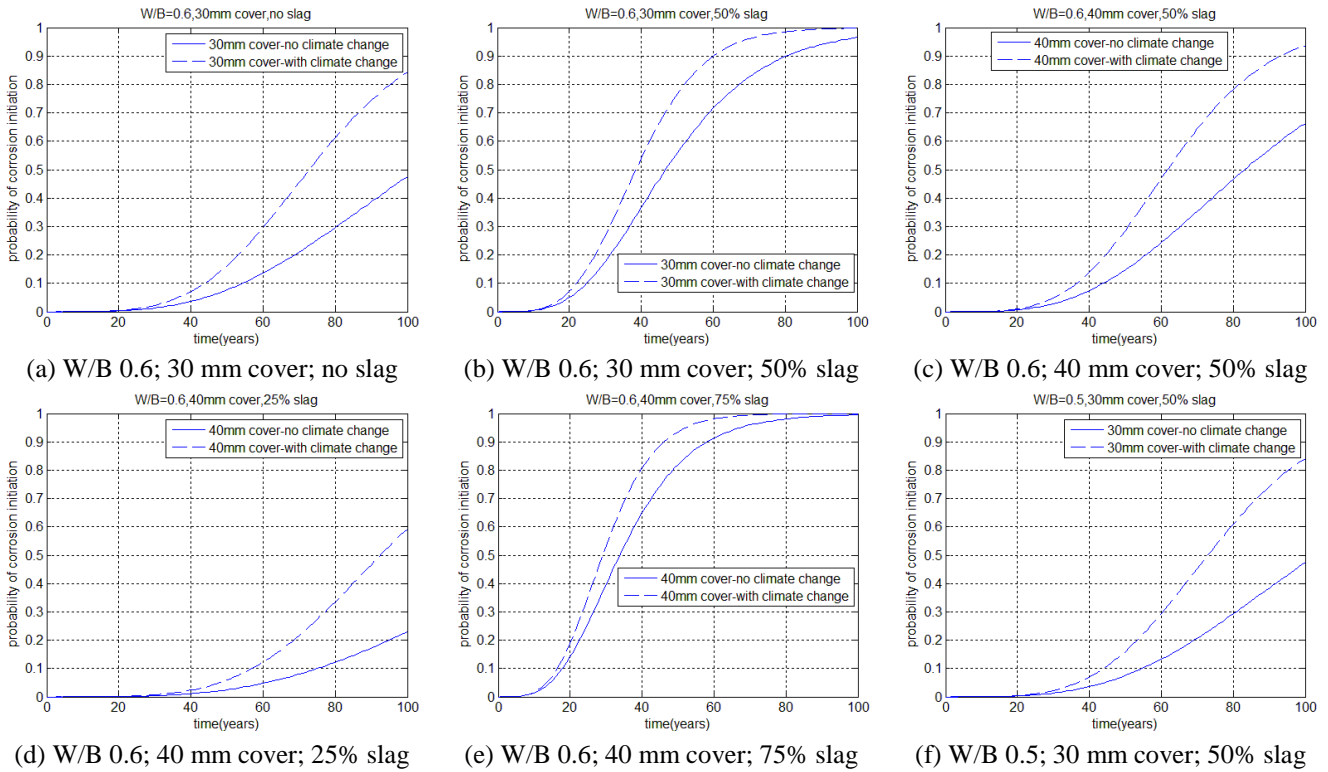


Fig. 6 Probability of corrosion initiation

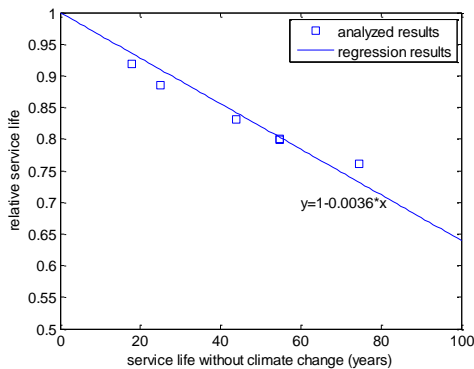
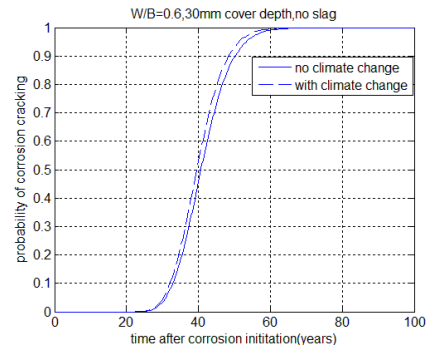


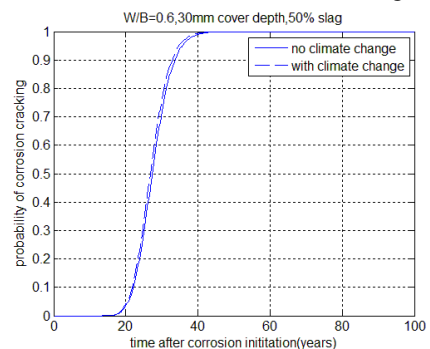
Fig. 7 Service life in corrosion initiation stage

Once the carbonation depth exceeds concrete cover depth, corrosion propagation period initiates. By using corrosion current density and Faraday’s law, the corroded depth of steel can be calculated. Furthermore, based on critical steel corrosion and Monte Carlo method, the probability of corrosion cracking can be determined. The compressive strength of slag blended concrete is evaluated using kinetic blended cement hydration model in our former study (Wang and Lee 2010).

Fig. 8 shows the probability of corrosion cracking considering the effects of climate change. Compared with corrosion initiation period (shown in Fig. 6), the effect of climate change on corrosion propagation period is small. The increase of probability of corrosion cracking due to climate change is marginal. This is because in corrosion initiation period, both CO<sub>2</sub> concentration increase and temperature increase affect the probability of durability failure. While in the corrosion propagation period, only



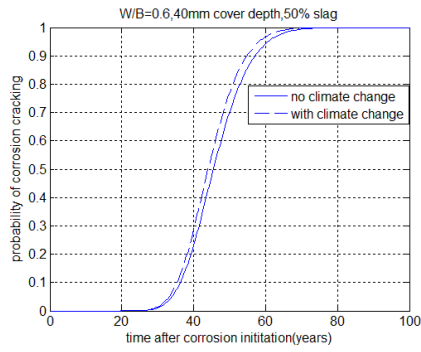
(a) W/B 0.6; 30 mm cover; no slag



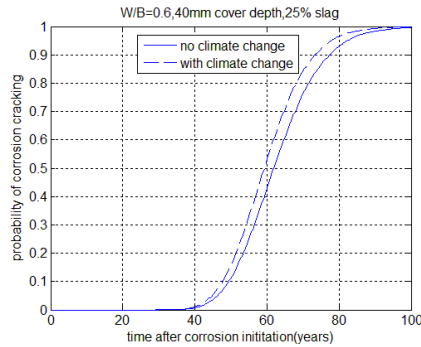
(b) W/B 0.6; 30 mm cover; 50% slag

Fig. 8 Probability of corrosion cracking

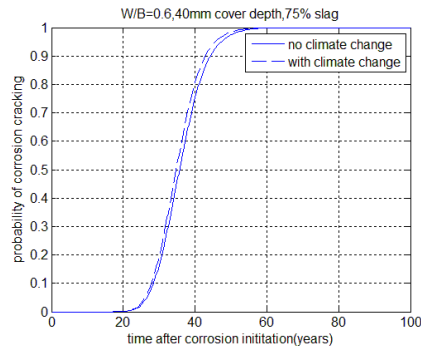
temperature increase affects the probability of durability failure. Slag additions will increase the probability of corrosion cracking (from Fig. 8(a) to Fig. 8(b), from Fig. 8(c) to Fig. 8(e)). When cover depth increases, the probability of corrosion cracking decreases (from Fig. 8(b)



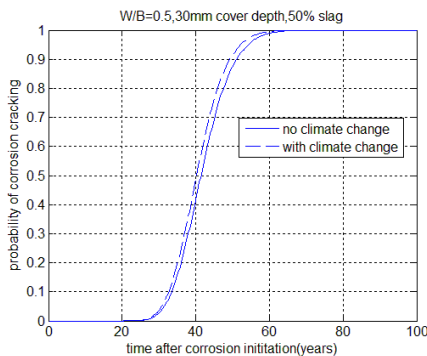
(c) W/B 0.6; 40 mm cover; 50% slag



(d) W/B 0.6; 40 mm cover; 25% slag



(e) W/B 0.6; 40 mm cover; 75% slag



(f) W/B 0.5; 30 mm cover; 50% slag

Fig. 8 Continued

to Fig. 8(c)). When water to binder ratio decreases (from Fig. 8(b) to Fig. 8(f)), the probability of corrosion cracking decreases.

In corrosion propagation period, the service life is the time required to achieve failure probability 7%. Based on the relation between time and probability of corrosion cracking, the service life is calculated and shown in Table 4.

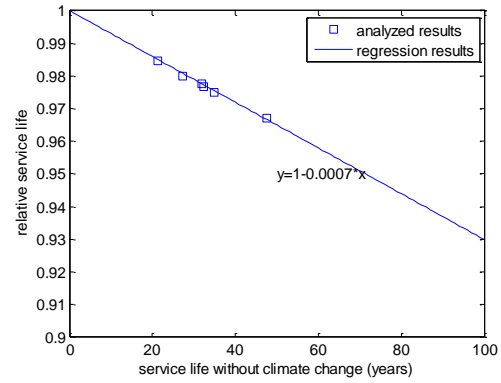


Fig. 9 service life in corrosion propagation stage

Table 3 Service life in corrosion initiation Stage

W/B	Cover depth (mm)	Slag replacement ratio	Service life in corrosion initiation Stage (years)		
			No climate change	With Climate change	Relative ratio
0.6	30	0	54.61	43.75	0.801
0.6	30	0.5	24.89	22.05	0.885
0.6	40	0.5	43.98	36.58	0.831
0.6	40	0.25	74.61	56.89	0.761
0.6	40	0.75	17.89	16.43	0.918
0.5	30	0.5	54.77	43.78	0.799

The reduction of service life due to climate change is less than 5%. Fig. 9 shows the relative service life as a function of former service life. The slope of linear regression equation of relative service life is -0.0007, which is much less than that shown in Fig. 7. In other words, climate change presents more significant influence on corrosion initiation period than on corrosion propagation period.

### 3.4 Whole service life of slag blended concrete

The whole service life equals the sum of service lives in corrosion initiation period and corrosion propagation period. By using the results shown in Table 3 (service life in corrosion initiation period) and in Table 4 (service life in corrosion propagation period), the whole service life is calculated and shown in Table 5. When former service life increases, relative service life decreases. Fig. 10 shows the relative service life as a function of former service life. The slope of linear regression equation of relative service life is -0.0014, which is between that of Fig. 7 and Fig. 9. For concrete with a former service life 50 years, after considering climate change, 7% service life reduces. In addition, in our recent study (Park and Wang 2017), we found that for high volume fly ash blended concrete with a 50 years former service life, after considering climate change, about 6% service life reduces, which is very similar to the calculation results shown in this study (7%). In other words, although the former service life of slag blended concrete is different from that of fly ash blended concrete, when relative service life is concerned, the influence of climate change on the reduction of relative service life is similar.

Table 4 Service life in corrosion propagation Stage

W/B	Cover depth (mm)	Slag replacement ratio	Service life in corrosion propagation Stage (years)		
			No climate change	With Climate change	Relative ratio
0.6	30	0	31.82	31.11	0.977
0.6	30	0.5	21.35	21.02	0.984
0.6	40	0.5	35.02	34.14	0.974
0.6	40	0.25	47.65	46.09	0.967
0.6	40	0.75	27.41	26.85	0.979
0.5	30	0.5	32.42	31.67	0.976

Table 5 Service life of concrete

W/B	Cover depth (mm)	Slag replacement ratio	Service life (years)		
			No climate change	With Climate change	Relative ratio
0.6	30	0	86.44	74.86	0.866
0.6	30	0.5	46.24	43.08	0.931
0.6	40	0.5	79.00	70.72	0.895
0.6	40	0.25	122.27	102.89	0.841
0.6	40	0.75	45.30	43.29	0.955
0.5	30	0.5	87.20	75.45	0.865

### 3.5 Discussion of proposed model

This study proposed a probabilistic numerical procedure for evaluating service life of slag blended concrete considering climate changes. After inputting the parameters (concrete mixing proportions, curing conditions, and climate change scenario), the service life can be calculated automatically. Based on this probabilistic numerical procedure, we can obtain a clear answer about the extent of service life reduction due to climate change.

The new contributions of this study are summarized as follows: First, the blended hydration model considers the effects of water to binder ratios and slag replacement levels on reaction degrees of binders. Second, this study considers the influences of slag replacement levels on carbonatable substance contents, concrete porosity, corrosion current density, and relative service life. Third, this study considers the difference in reliability index between corrosion initiation period and corrosion propagation period. In addition, CO<sub>2</sub> can be absorbed by concrete due to carbonation reaction between CO<sub>2</sub> and carbonatable substances. The proposed model in this study can calculate the contents of carbonatable substance and carbonation depth, and the proposed model has a potential ability to calculate CO<sub>2</sub> uptake due to carbonation.

However, the study has some limitations. The limitations of this study are summarized as follows: First, the proposed model does not consider the moisture diffusion during carbonation of concrete. The produced water from carbonation may affect concrete relative humidity. Second, corrosion current density may decrease with exposure time due to the filling effect of corrosion products and the decrease of oxygen diffusivity. This point is not considered in this study. Third, for real concrete structures, transverse crack exists in the tensile zone of

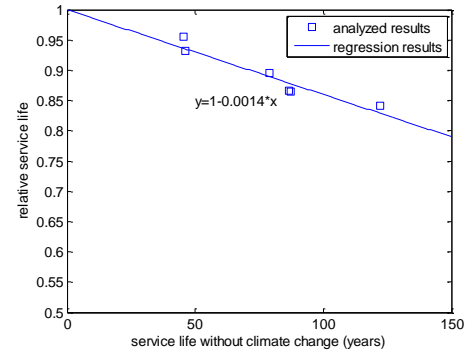


Fig. 10 whole service life

concrete. This study does not consider the influences of transverse crack on oxygen diffusivity and corrosion current density.

## 4. Conclusions

This study presents a probabilistic numerical procedure for evaluating the carbonation service life of slag blended concrete considering climate changes. The input parameters consist of concrete mixing proportions, curing conditions, and climate change scenario. This numerical procedure considers both corrosion initiation period and corrosion propagation period.

In corrosion initiation period, by using a hydration-carbonation integrated model, the carbonation depth is calculated considering time-dependent CO<sub>2</sub> concentration and environmental temperature. Furthermore, the probability of corrosion initiation is determined using Monte-Carlo method. In initiation period, the service life is the time required to achieve failure probability 10%. Relative service life approximately linearly decreases with the increase of former service life.

In corrosion propagation period, based on critical steel corrosion and the progress of degree of corrosion, the probability of surface concrete cracking is determined. In corrosion propagation period, the service life is the time required to achieve failure probability 7%. Climate change presents more significant influence on corrosion initiation period than on corrosion propagation period.

The whole service life equals the sum of service lives in corrosion initiation period and corrosion propagation period. When former service life increases, relative service life decreases. The analysis results show that for concrete structures with 50 years service life, after considering climate changes, the service life reduces about 7%.

## Acknowledgments

This research was supported by the Basic Science Research Program through the National Research Foundation of Korea (NRF), funded by the Ministry of Science, ICT and Future Planning (No. 2015R1A5A1037548) and a NRF grant (NRF-2017R1C1B1010076).

## References

- Bastidas-Arteaga, E., Schoefs, F., Stewart, M.G. and Wang, X.M. (2013), "Influence of global warming on durability of corroding RC structures: A probabilistic approach", *Eng. Struct.*, **51**, 259-266.
- Bentz, D.P. (2005), *CEMHYD3D: A Three-Dimensional Cement Hydration and Microstructure Development Modeling Package*, Version 3.0, NISTIR 7232.
- Bentz, D.P. and Remold, S. (1997), *Incorporation of Fly Ash into a 3-D Cement Hydration Microstructure Model*, NISTIR 6050.
- Damtoft, J.S., Lukasik, J., Herfort, D., Sorrentino, D. and Gartner, E.M. (2008), "Sustainable development and climate change initiatives", *Cement Concrete Res.*, **38**(2), 115-127.
- FIB (2006), Model Code for Service Design, International Federation of Structural Concrete, Switzerland.
- Garcia-Segura, T., Yepes, V. and Alcala, J. (2014), "Life cycle greenhouse gas emissions of blended cement concrete including carbonation and durability", *Int. J. Life Cycle Assess.*, **19**(1), 3-12.
- Geng, O. (2010), *Reinforcement Corrosion and Degradation Rate of Concrete Members*, China Railway Publishing House.
- Gruyaert, E., den Heede, P.V. and De Belie, N. (2013), "Carbonation of slag concrete: Effect of the cement replacement level and curing on the carbonation coefficient-Effect of carbonation on the pore structure", *Cement Concrete Compos.*, **35**(1), 39-48.
- Houghton, J.T., Ding, Y., Griggs, D.J., Noguier, M., van der Linden, P.J., Dai, X., Maskell, K. and Johnson, C.A. (2001), *Climate Change 2001: The Scientific Basis*, Cambridge University Press.
- Isgor, O.B. and Razaqpur, A.G. (2004), "Finite element modeling of coupled heat transfer, moisture transport and carbonation processes in concrete structures", *Cement Concrete Compos.*, **26**(1), 57-73.
- Khunthongkeaw, J., Tangtermsirikul, S. and Leelawat, T. (2006), "A study on carbonation depth prediction for fly ash concrete", *Constr. Build. Mater.*, **20**(9), 744-753.
- Kolio, A., Pakkala, T.A., Lahdensivu, J. and Kiviste, M. (2014), "Durability demands related to carbonation induced corrosion for Finnish concrete buildings in changing climate", *Eng. Struct.*, **62**, 42-52.
- Kwon, S.J. and Na, U.J. (2011), "Prediction of durability for RC columns with crack and joint under carbonation based on probabilistic approach", *Int. J. Concrete Struct. Mater.*, **5**(1), 11-18.
- Larrarda, T., Bastidas-Arteaga, E., Duprat, F. and Schoefs, F. (2014), "Effects of climate variations and global warming on the durability of RC structures subjected to carbonation", *Civil Eng. Environ. Syst.*, **31**(2), 153-164.
- Marques, P.F., Chastre, C. and Nunes, A. (2013), "Carbonation service life modelling of RC structures for concrete with Portland and blended cements", *Cement Concrete Compos.*, **37**, 171-184.
- Marques, P.F., Costa, A. and Lanata, F. (2012), "Service life of RC structures: chloride induced corrosion: prescriptive versus performance-based methodologies", *Mater. Struct.*, **45**(1), 277-296.
- Papadakis, V.G. (2000), "Effect of supplementary cementing materials on concrete resistance against carbonation and chloride ingress", *Cement Concrete Res.*, **30**(2), 291-299.
- Papadakis, V.G. (2007), "Computer-aided approach of parameters influencing concrete service life and field validation", *Comput. Concrete*, **4**(1), 1-18.
- Park, K.B. and Wang, X.Y. (2017), "Effect of climate change on service life of high volume fly ash concrete subjected to carbonation-A Korean case study", *Sustainab.*, **9**(1), 157-172.
- Parrott, L.J. (1994), "A study of carbonation-induced corrosion", *Mag. Concrete Res.*, **46**(166), 23-28.
- Parrott, L.J. (1996), "Some effects of cement and curing upon carbonation and reinforcement corrosion in concrete", *Mater. Struct.*, **29**(3), 164-173.
- Peng, L. and Stewart, M.G. (2014), "Spatial time-dependent reliability analysis of corrosion damage to RC structures with climate change", *Mag. Concrete Res.*, **66**(22), 1154-1169.
- Peng, L. and Stewart, M.G. (2016), "Climate change and corrosion damage risks for reinforced concrete infrastructure in China", *Struct. Infrastr. Eng.*, **12**(4), 499-516.
- Sisomphon, K. and Franke, L. (2007), "Carbonation rates of concretes containing high volume of pozzolanic materials", *Cement Concrete Res.*, **37**(12), 1647-1653.
- Stewart, M.G., Wang, X.M. and Nguyen, M.N. (2011), "Climate change impact and risks of concrete infrastructure deterioration", *Eng. Struct.*, **33**(4), 1326-1337.
- Sulapha, P., Wong, S.F., Wee, T.H. and Swaddiwudhipong, S. (2003), "Carbonation of concrete containing mineral admixtures", *J. Mater. Civil Eng.*, **15**(2), 134-143.
- Talukdar, S., Grace, J. and Banthia, N. (2012), "The effects of structural cracking on carbonation progress in reinforced concrete: is climate change a concern?", *Proceedings of the 3<sup>rd</sup> International Conference on the Durability of Concrete Structures*, Queen's university Belfast.
- Talukdar, S., Grace, J., Banthia, N. and Cohen, S. (2014), "Climate change-induced carbonation of concrete infrastructure", *Proc. Inst. Civil Eng. Constr. Mater.*, **167**(3), 140-150.
- Wang, X.Y. (2010), "A hydration-based integrated system for blended cement to predict the early-age properties and durability of concrete", Ph.D. Thesis, Hanyang University, Korea.
- Wang, X.Y. and Lee, H.S. (2010), "Modeling the hydration of concrete incorporating fly ash or slag", *Cement Concrete Res.*, **40**(7), 984-996.
- Wei, J., Meng, H. and Xue, S.G. (2011), "FEM analysis on the crack process of concrete cover induced by non-uniform corrosion of re-bar", *J. Xi'an Univ. Arch. Technol.*, **43**(5), 747-754.
- Yoon, I.S., Copuroglua, O. and Park, K.B. (2007), "Effect of global climatic change on carbonation progress of concrete", *Atmosph. Environ.*, **41**(34), 7274-7285.

CC